Acta Cryst E CRYSTALLOGRAPHIC COMMUNICATIONS

ISSN 2056-9890

(*E*)-{[(Butylsulfanyl)methanethioyl]amino}(4-methoxybenzylidene)amine: crystal structure and Hirshfeld surface analysis

Aqilah Fasihah Rusli,[a] Huey Chong Kwong,[a] Karen A. Crouse,[a]‡ Mukesh M. Jotani[b] and Edward R. T. Tiekink[c]*

[a]Department of Chemistry, Faculty of Science, Universiti Putra Malaysia, UPM, Serdang 43400, Malaysia, [b]Department of Physics, Bhavan's Sheth R. A. College of Science, Ahmedabad, Gujarat 380001, India, and [c]Research Centre for Crystalline Materials, School of Science and Technology, Sunway University, 47500 Bandar Sunway, Selangor Darul Ehsan, Malaysia. *Correspondence e-mail: edwardt@sunway.edu.my

Received 8 January 2020
Accepted 12 January 2020

Edited by W. T. A. Harrison, University of Aberdeen, Scotland

‡ Additional correspondence author, e-mail: kacrouse@gmail.com.

Keywords: crystal structure; Schiff base; hydrazine carbodithioate; hydrogen bonding; Hirshfeld surface analysis.

CCDC reference: 1977066

Supporting information: this article has supporting information at journals.iucr.org/e

The title hydrazine carbodithioate, $C_{13}H_{18}N_2OS_2$, is constructed about a central and almost planar $C_2N_2S_2$ chromophore (r.m.s. deviation = 0.0263 Å); the terminal methoxybenzene group is close to coplanar with this plane [dihedral angle = 3.92 (11)°]. The *n*-butyl group has an extended all-*trans* conformation [torsion angles S—C_m—C_m—C_m = −173.2 (3)° and C_m—C_m—C_m—C_{me} = 180.0 (4)°; m = methylene and me = methyl]. The most prominent feature of the molecular packing is the formation of centrosymmetric eight-membered $\{\cdots HNCS\}_2$ synthons, as a result of thioamide-N—H···S(thioamide) hydrogen bonds; these are linked *via* methoxy-C–H···π(methoxybenzene) interactions to form a linear supramolecular chain propagating along the *a*-axis direction. An analysis of the calculated Hirshfeld surfaces and two-dimensional fingerprint plots point to the significance of H···H (58.4%), S···H/H···S (17.1%), C···H/H···C (8.2%) and O···H/H···O (4.9%) contacts in the packing. The energies of the most significant interactions, *i.e.* the N—H···S and C—H···π interactions have their most significant contributions from electrostatic and dispersive components, respectively. The energies of two other identified close contacts at close to van der Waals distances, *i.e.* a thione–sulfur and methoxybenzene–hydrogen contact (occurring within the chains along the *a* axis) and between methylene-H atoms (occurring between chains to consolidate the three-dimensional architecture), are largely dispersive in nature.

1. Chemical context

The dithiocarbazate dianion, NH_2NHCS^{2-}, and its esters such as *S*-benzyldithiocarbazate (Tian *et al.*, 1996) and *S*-methyldithiocarbazate (Ali *et al.*, 2008), are well-known to function as starting materials for the synthesis of a wide variety of Schiff bases containing both hard nitrogen and soft sulfur donor atoms. Schiff bases derived from *S*-alkyl esters of dithiocarbazate, $NH_2NHC(=S)SR$, and their metal complexes have been the subject of many studies because of their ability to act as multidentate ligands to metals and the subsequent enhanced bioactivity upon complexation (Bera *et al.*, 2009; Ali *et al.*, 2012; Begum *et al.*, 2017). Schiff bases derived from the condensation of *S*-methyl- or *S*-benzyldithiocarbazate with heterocyclic aldehydes and ketones can complex metals to form five-membered chelate rings with the metal atoms bound to nitrogen and sulfur atoms (Ali *et al.*, 2003) while complexation *via* two sulfur atoms, resulting in the formation of a four-membered chelate ring, is also possible (Rakha & Bekheit, 2000). It is also known that slight changes in mol-

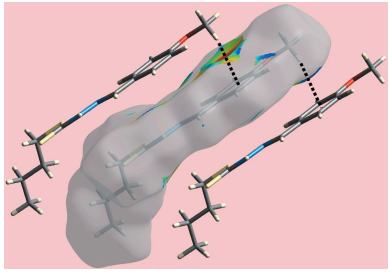

ecular structure can give rise to different coordination geometries (Chan *et al.*, 2008). In a continuation of structural studies of *S*-alkyl dithiocarbazate esters (Yusof *et al.*, 2015; Low *et al.*, 2016; Omar *et al.*, 2018) and their complexation to metals with accompanying evaluation of biological potential (Low *et al.*, 2016; Ravoof *et al.*, 2017; Yusof *et al.*, 2017), herein the crystal and molecular structures of the title hydrazine carbodithioate ester, (I), along with the calculated Hirshfeld surfaces and computational chemistry are described.

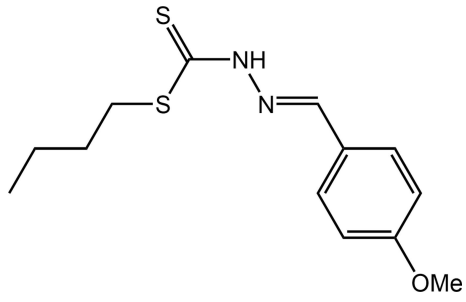

2. Structural commentary

The molecular structure of (I), Fig. 1, features a central $C_2N_2S_2$ residue which is close to planar, as seen in the r.m.s. deviation of 0.0263 Å for the fitted atoms. The maximum deviations to opposite sides of the plane occur for the N1 [0.0393 (18) Å] and C2 [0.0388 (14) Å] atoms with the appended C3 [0.033 (3) Å] and C10 [0.089 (4) Å] atoms lying to the same side of the central plane as the C2 atom. The methoxybenzene ring forms a dihedral angle of 3.92 (11)° with the central residue indicating a close to co-planar relationship. The C9—O1—C6 —C7 dihedral angle of 176.9 (3)° indicates that the methoxy substituent lies almost in the plane of the benzene ring to which it is connected. The configuration about the C2═N2 imine bond [1.278 (3) Å] is *E* and this bond length is significantly shorter than the C1—N1 bond [1.330 (3) Å]; the N1—N2 bond length is 1.378 (3) Å. There is a large disparity in the C1—S1 [1.662 (3) Å] and C1—S2 [1.745 (3) Å] bond lengths, which correlate with significant double-bond character in the former; the C10—S2 bond length at 1.793 (3) Å is longer than each of these. The thione character of the C1—S1 bond is also reflected in the range of angles subtended at the C1 atom, which are systematically wider for those involving the thione-S1 atom, *i.e.* S1—C1—S2 [126.35 (16)°] and S1—C1—N1 [120.9 (2)°], *cf.* S2—C1—N1 [112.76 (19)°]. The thioamide-N—H and thioamide-S atoms have a *syn* disposition. Finally, the *n*-butyl group has an extended, all-*trans* conformation as seen in the S2—C10—C11—C12 [−173.2 (3)°] and C10—C11—C12—C13 [180.0 (4)°] torsion angles.

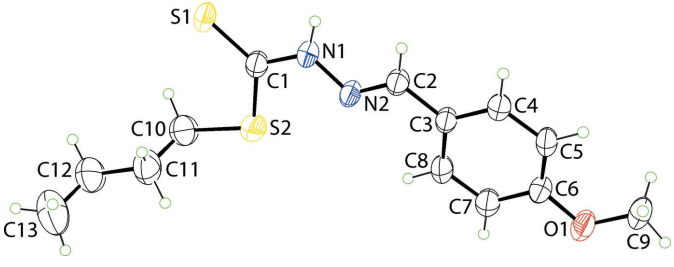

Figure 1
The molecular structure of (I) showing the atom-labelling scheme and displacement ellipsoids at the 35% probability level.

3. Supramolecular features

With the exception of thioamide-N—H···S(thioamide) hydrogen bonding between centrosymmetrically related molecules, Table 1, and which sustain a dimeric aggregate *via* an eight-membered $\{\cdots HNCS\}_2$ synthon, the molecular packing is largely devoid of directional interactions (Spek, 2020). The

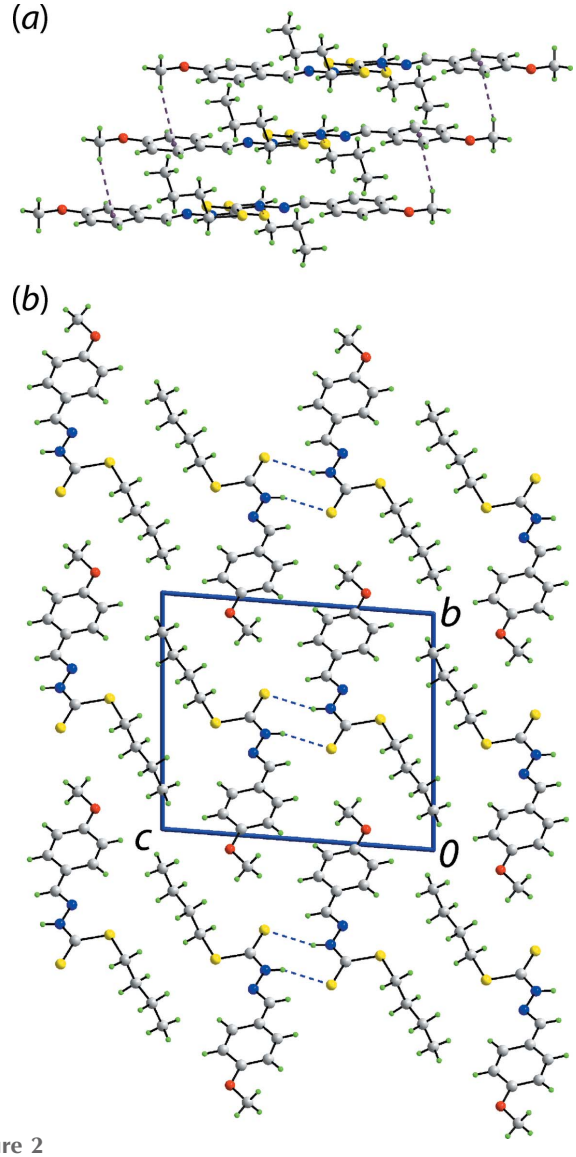

Figure 2
Molecular packing in (I): (*a*) the linear supramolecular chain whereby dimeric aggregates sustained by thioamide-N—H···S(thioamide) hydrogen bonding, shown by blue dashed lines, are connected by methoxy-C—H···π interactions (purple dashed lines) and (*b*) a view of the unit-cell contents shown in projection down the *a* axis highlighting the stacking of dimeric aggregates.

Table 1
Hydrogen-bond geometry (Å, °).

*Cg*1 is the centroid of the (C3–C8) ring.

D—H···*A*	*D*—H	H···*A*	*D*···*A*	*D*—H···*A*
N1—H1*N*···S1^{i}	0.86 (1)	2.61 (2)	3.425 (3)	160 (3)
C9—H9*C*···*Cg*1^{ii}	0.96	2.98	3.748 (4)	138

Symmetry codes: (i) $-x+1, -y+1, -z+1$; (ii) $x+1, y, z$.

dimeric aggregates are connected into a linear supramolecular chain along the *a*-axis direction *via* weak methoxy-C—H···π(methoxybenzene) interactions, Fig. 2(*a*), being the only other identified supramolecular association. Globally, chains pack without specific interactions between them, Fig. 2(*b*). An analysis of the weak non-covalent contacts within and connecting chains is given in the *Analysis of the Hirshfeld surfaces*.

4. Analysis of the Hirshfeld surfaces

The calculation of the Hirshfeld surfaces for (I) were conducted as per a literature precedent (Tan *et al.*, 2019) employing *Crystal Explorer 17* (Turner *et al.*, 2017). The presence of bright-red spots near the thioamide-S1 and H1*N* atoms on the Hirshfeld surface mapped over d_{norm} shown in Fig. 3 reflect the intermolecular N—H···S hydrogen bonding.

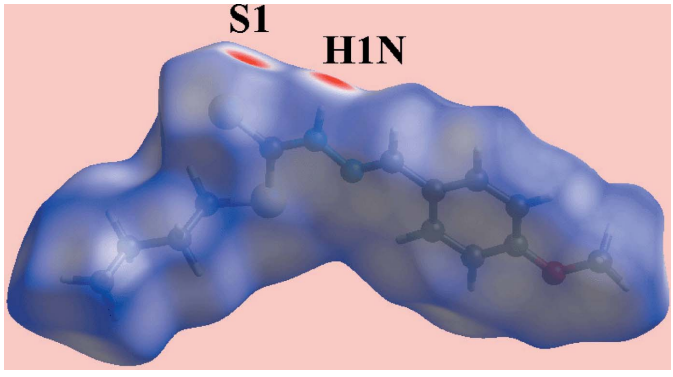

Figure 3
A view of the Hirshfeld surface for (I) mapped over d_{norm} in the range −0.299 to +1.278 arbitrary units.

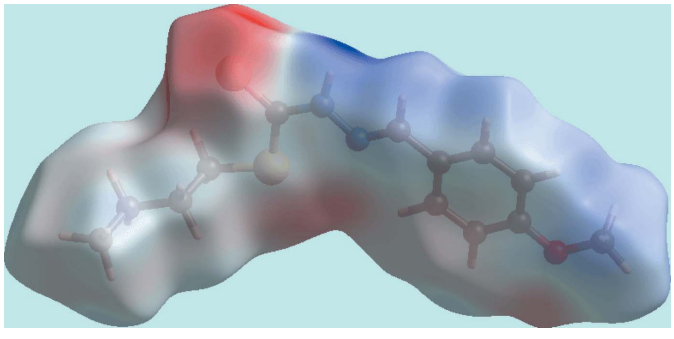

Figure 4
A view of the Hirshfeld surface for (I) mapped over the electrostatic potential in the range −0.056 to +0.104 atomic units.

Table 2
The percentage contributions of interatomic contacts to the Hirshfeld surface for (I).

Contact	Percentage contribution
H···H	58.4
S···H/H···S	17.1
C···H/H···C	8.2
O···H/H···O	4.9
C···N/N···C	4.2
C···C	3.0
S···N/N···S	1.7
N···H/H···N	0.9
C···O/O···C	0.9
C···S/S···C	0.7

The donor and acceptor associated with this interaction are also viewed as the blue and red regions, corresponding to positive and negative electrostatic potentials, respectively, on the Hirshfeld surface mapped over the calculated electrostatic potential in Fig. 4. The intermolecular methoxy-C—H···π(methoxybenzene) interaction is also evident in Fig. 4, as the light-blue and light-red regions around the participating atoms. Fig. 5 also illustrates the donors and acceptors of this C—H···π contact through the dotted lines connecting the blue bump and red concave regions, respectively, on the Hirshfeld surface mapped with the shape-index property.

The overall two-dimensional fingerprint plot for (I) along with those delineated into the individual H···H, S···H/H···S, C···H/H···C and O···H/H···O contacts are illustrated in Fig. 6(*a*)–(*e*), respectively; the percentage contributions from the different interatomic contacts are summarized in Table 2. In the fingerprint plot delineated into H···H contacts, Fig. 6(*b*), a short interatomic H···H contact involving methylene-H10*B* with a symmetry-related mate (H10*B*···H10*B* = 2.26 Å; symmetry operation $-x, 1-y, 2-z$) and occurring between supramolecular chains aligned along the *a* axis, is observed as a single peak at $d_e + d_i \sim 2.2$ Å. In the fingerprint delineated into S···H/H···S contacts, shown in

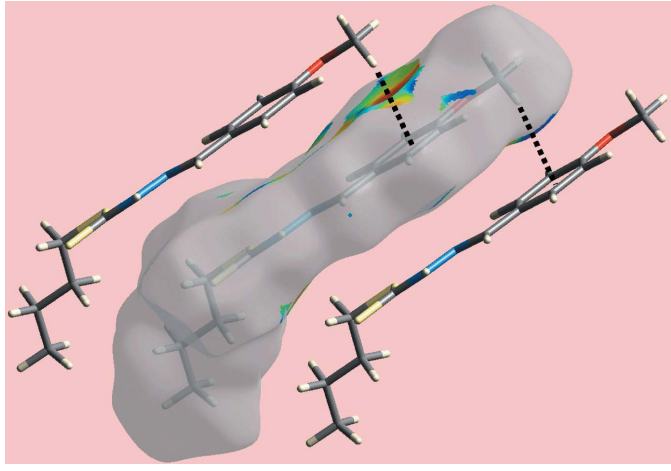

Figure 5
A view of the Hirshfeld surface with the shape-index property highlighting the donors and acceptors of the C—H···π/π···H—C contacts by black dotted lines.

Table 3
A summary of interaction energies (kJ mol^{-1}) calculated for (I).

Contact	R (Å)	E_{ele}	E_{pol}	E_{dis}	E_{rep}	E_{tot}
N1—H1*N*···S1^{i}	8.17	−59.2	−10.3	−17.1	66.6	−43.9
C9—H9*C*···*Cg*(C3–C8)^{ii}	4.71	−2.2	−3.8	−64.0	35.9	−38.8
S1···H4^{iii}	6.85	−15.6	−5.2	−19.3	19.6	−25.1
H10*B*···H10*B*^{iv}	10.74	−1.0	−0.3	−11.3	5.7	−7.5

Symmetry codes: (i) $1-x, 1-y, 1-z$; (ii) $1+x, y, z$; (iii) $2-x, 1-y, 1-z$; (iv) $-x, 1-y, 2-z$.

Fig. 6(*c*), the pair of well-defined spikes at $d_e + d_i \sim 2.5$ Å arise as a result of the prominent intermolecular N—H···S interaction. The points corresponding to S···H/H···S contacts involving the thione-S1 and methoxybenzene-H4 atoms, occurring within the supramolecular chain shown in Fig. 2(*a*), albeit at nearly van der Waals separations (S1···H4 = 3.02 Å for $2-x, 1-y, 1-z$), and reflected as an electrostatic interaction in the Hirshfeld surface plotted over the electrostatic potential of Fig. 4, are merged within the plot. Although the points in the fingerprint plot delineated into C···H/H···C contacts in Fig. 6(*d*) are at distances equal to or greater than the sum of van der Waals radii, the presence of characteristic wings is the result of the intermolecular methyoxy-C—H···π(methoxybenzene) contact. The points corresponding to interatomic O···H/H···O contacts illustrated in the corresponding fingerprint plot of Fig. 6(*e*), also show a pair of forceps-like tips at $d_e + d_i \sim 2.8$ Å, *i.e.* at van der Waals distances. The contribution from the other interatomic contacts summarized in Table 2 have negligible influence on the calculated Hirshfeld surface of (I).

5. Computational chemistry

The pairwise interaction energies between molecules in the crystal of (I) were calculated by summing up four energy components, comprising electrostatic (E_{ele}), polarization (E_{pol}), dispersion (E_{dis}) and exchange-repulsion (E_{rep}) (Turner *et al.*, 2017); the energies were calculated using the wave function calculated at the B3LYP/6-31G(*d*,p) level of theory. The nature and strength of the intermolecular interactions in terms of their energies are quantitatively summarized in Table 3. As indicated in Table 3, the electrostatic energy component is most significant for the N—H···S hydrogen bond but also makes a significant contribution to the thione-S1 and methoxybenzene-H4 contact, nearly as great as the dispersive component. The other two intermolecular interactions listed in Table 3 show major contributions from dispersion to the energy. The most stabilizing interactions, in

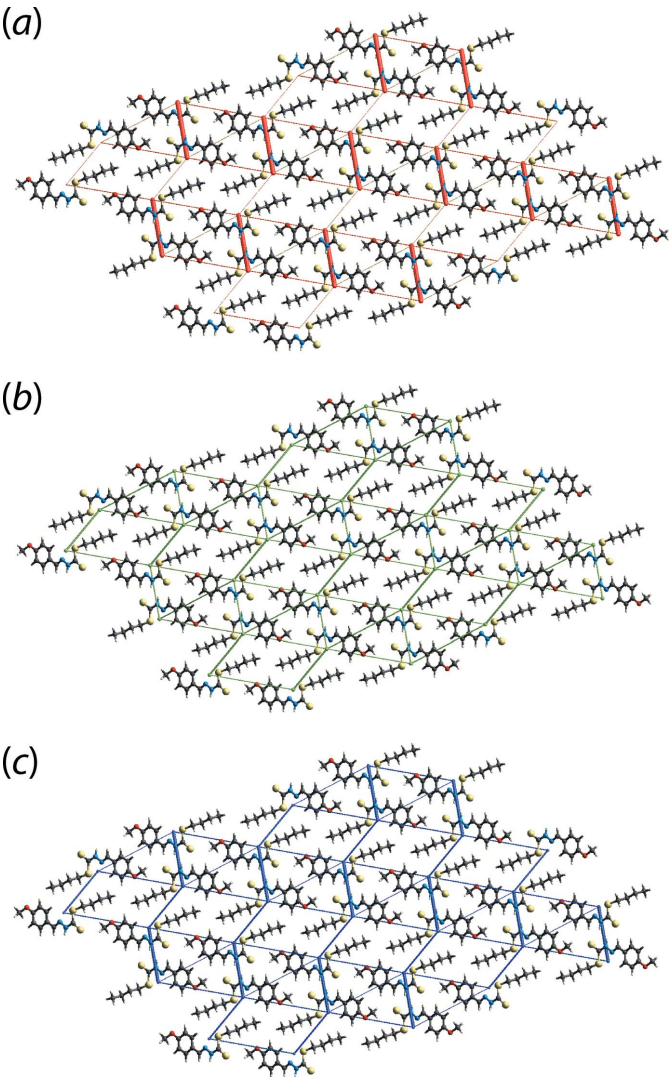

Figure 7
The calculated energy frameworks viewed down the *a*-axis direction comprising (*a*) electrostatic potential force, (*b*) dispersion force and (*c*) total energy for a cluster about a reference molecule of (I). The energy frameworks were adjusted to the same scale factor of 50 with a cut-off value of 3 kJ mol^{-1} within 4 × 4 × 4 unit cells.

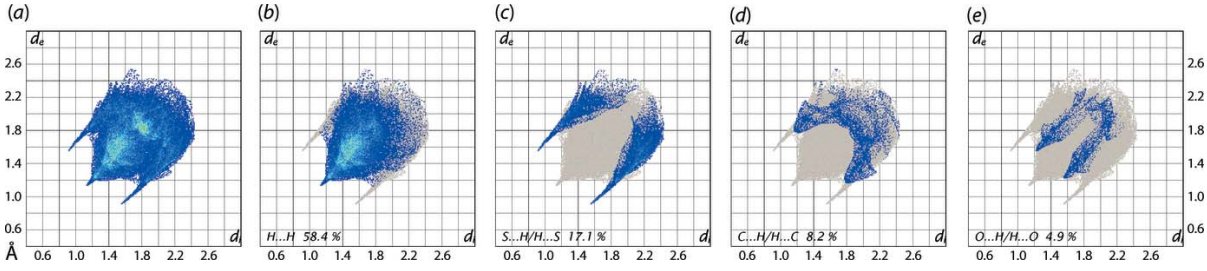

Figure 6
(*a*) The full two-dimensional fingerprint plot for (I) and fingerprint plots delineated into (*b*) H···H, (*c*) S···H/H···S, (*d*) C···H/H···C and (*e*) O···H/H···O contacts.

order, are those arising from the N—H···S and C—H···π contacts, compared to the short interatomic S···H/H···S and H···H contacts. The magnitudes of intermolecular energies are also represented graphically in Fig. 7 by energy frameworks in order to view the supramolecular architecture of the crystal through cylinders that connect the centroids of molecular pairs. This is done using red, green and blue colour codes for the E_{ele}, E_{disp} and E_{tot} components, respectively; the radius of the cylinder is proportional to the magnitude of the interaction energies. This is reflected in the relatively thick red cylinders corresponding to the electrostatic interactions *via* the N—H···S hydrogen bonding in Fig. 7(*a*) and the thick green cylinders corresponding to the strong dispersive interactions provided by the methyoxy-C—H···π(methoxy-(methoxybenzene) interactions in Fig. 7(*b*).

6. Database survey

Reflecting the interest in the chemistry of hydrazine carbodithioates related to (I), there are four crystal structures of literature precedents of the general formula, 4-MeOC$_6$H$_4$C(H)═NN(H)C(═S)S*R*. These are of the *R* = Me (CCDC refcode ZITZIL; Fun *et al.*, 1996), *n*-hexyl (HUDJOH; Begum, Howlader *et al.*, 2015), *n*-ocyl (XUFPAR; Begum, Zangrando *et al.*, 2015) and CH$_2$Ph (YAHDAO; Fan *et al.*, 2011) compounds. The common feature of all five structures is the *E*-configuration about the imine bond and the *syn* relationship between the thioamide-N—H and thioamide-S atoms in their molecular structures. Further, the formation of centrosymmetric, eight-membered {···HNCS}$_2$ synthons is common in their crystals. For the *n*-hexyl and *n*-octyl compounds, extended, all-*trans* conformations are found for the alkyl chains, as for (I).

7. Synthesis and crystallization

In an ice-bath, carbon disulfide (10.6 ml, 0.11 mol) was added dropwise to an absolute ethanol (35 ml) solution comprising KOH (6.2 g, 0.11 mol) and hydrazine hydrate (5.7 ml, 0.11 mol). After 30 min, 1-bromobutane (20 ml, 0.11 mol) was added. The solution was stirred at 278 K for 1 h to form *S*-butyldithiocarbazate (SBuDTC). An ethanolic solution (28 ml) of 4-methoxybenzaldehyde (16.8 ml, 0.11 mol) was added directly to the SBuDTC *in situ*. This mixture was heated to 323 K with continuous stirring for 30 min. The yellow product (I) was filtered, washed with water and dried under vacuum. Colourless blocks suitable for the X-ray analysis were obtained from an ethanol solution of (I) by slow evaporation. Yield: 0.18 g, 65%. M.p. 375.7–376.3 K. Analysis calculated: C$_{13}$H$_{18}$N$_2$OS$_2$: C, 55.3; H, 6.4; N, 9.9; S, 22.7. Found: C, 55.9; H, 6.6; N, 9.8; S, 23.2. FT–IR (cm^{-1}): 3120 ν(NH), 2927 ν(CH), 1600 ν(C═N), 1248 and 1107 ν(COC), 1017 ν(NN), 861 ν(CSS). MS: calculated *m*/*z* = 282; Found *m*/*z* = 282. ^{1}H NMR (DMSO-*d*$_6$; 500 MHz): δ 13.11 (1H, *s*, NH), 8.15 (1H, *s*, CH═N), 6.97, 7.02, 7.61, 7.78 (ArH), 3.76 (3H, *s*, OCH$_3$), 3.14 (2H, *t*, SCH$_2$), 1.58 (2H, *q*, CH$_2$), 1.36 (2H, sextet, CH$_2$), 0.86 (3H, *t*, CH$_3$). ^{13}C{^{1}H} NMR (DMSO-*d*$_6$; 125 MHz): δ 196.96 (C═S), 146.87 (C═N), 161.90, 129.65, 126.36, 115.00 (ArC), 55.86 (OCH$_3$), 33.19, 31.05, 22.10 (CH$_2$), 14.07 (CH$_3$). NMR data were measured on a JOEL ECX500 FT NMR spectrometer.

Table 4
Experimental details.

Crystal data	
Chemical formula	C$_{13}$H$_{18}$N$_2$OS$_2$
M_r	282.41
Crystal system, space group	Triclinic, $P\overline{1}$
Temperature (K)	295
a, *b*, *c* (Å)	4.7131 (3), 11.6998 (8), 13.5696 (8)
α, β, γ (°)	85.225 (5), 81.139 (5), 87.379 (5)
V (Å^3)	736.35 (8)
Z	2
Radiation type	Mo *K*α
μ (mm^{-1})	0.35
Crystal size (mm)	0.30 × 0.25 × 0.20
Data collection	
Diffractometer	Agilent Technologies SuperNova Dual diffractometer with Atlas detector
Absorption correction	Multi-scan (*CrysAlis PRO*; Agilent, 2012)
T_{min}, T_{max}	0.868, 1.000
No. of measured, independent and observed [$I > 2\sigma(I)$] reflections	9986, 3395, 2244
R_{int}	0.029
(sin $\theta/\lambda)_{max}$ (Å^{-1})	0.651
Refinement	
$R[F^2 > 2\sigma(F^2)]$, $wR(F^2)$, *S*	0.055, 0.174, 1.03
No. of reflections	3395
No. of parameters	169
No. of restraints	1
H-atom treatment	H atoms treated by a mixture of independent and constrained refinement
$\Delta\rho_{max}$, $\Delta\rho_{min}$ (e Å^{-3})	0.52, −0.46

Computer programs: *CrysAlis PRO* (Agilent, 2012), *SHELXT2014* (Sheldrick, 2015*a*), *SHELXL2014* (Sheldrick, 2015*b*), *ORTEP-3 for Windows* (Farrugia, 2012), *DIAMOND* (Brandenburg, 2006) and *publCIF* (Westrip, 2010).

8. Refinement

Crystal data, data collection and structure refinement details are summarized in Table 4. The carbon-bound H atoms were placed in calculated positions (C—H = 0.93–0.97 Å) and were included in the refinement in the riding model approximation, with U_{iso}(H) set to 1.2U_{eq}(C). The N-bound H atom was located in a difference-Fourier map but was refined with a N—H distance restraint of 0.86 (1) Å.

Funding information

Financial support from the Ministry of Science, Technology and Innovation Malaysia and the Universiti Putra Malaysia (RUGS 05-01-11-1243RU and FRGS 01-13-11-986FR) as well as scholarships (MyBrain15 and Graduate Research Fellowship) for AFR are gratefully acknowledged. Crystallographic research at Sunway University is supported by Sunway University Sdn Bhd (grant No. STR-RCTR-RCCM-001-2019).

References

Agilent (2012). *CrysAlis PRO*. Agilent Technologies, Yarnton, England.

Ali, M. A., Mirza, A. H., Nazimuddin, M., Ahmed, R., Gahan, L. R. & Bernhardt, P. V. (2003). *Polyhedron* **22**, 1471–1479.

Ali, M. A., Mirza, A. H., Hamid, M. H. S. A., Bernhardt, P. V., Atchade, O., Song, X., Eng, G. & May, L. (2008). *Polyhedron*, **27**, 977–984.

Ali, M. A., Tan, A. L., Mirza, A. H., Santos, J. H. & Abdullah, A. H. (2012). *Transition Met. Chem.* **37**, 651–659.

Begum, M. S., Howlader, M. B. H., Miyatake, R., Zangrando, E. & Sheikh, M. C. (2015). *Acta Cryst.* E**71**, o199.

Begum, M. S., Zangrando, E., Sheikh, M. C., Miyatake, R. & Hossain, M. M. (2015). *Acta Cryst.* E**71**, o265–o266.

Begum, M. S., Zangrando, E., Sheikh, M. C., Miyatake, R., Howlader, M. B. H., Rahman, M. N. & Ghosh, A. (2017). *Transit. Met. Chem.* **42**, 553–563.

Bera, P., Kim, C.-H. & Seok, S. I. (2009). *Inorg. Chim. Acta*, **362**, 2603–2608.

Brandenburg, K. (2006). *DIAMOND*. Crystal Impact GbR, Bonn, Germany.

Chan, M. E., Crouse, K. A., Tahir, M. I. M., Rosli, R., Umar-Tsafe, N. & Cowley, A. R. (2008). *Polyhedron*, **27**, 1141–1149.

Fan, Z., Huang, Y.-L., Wang, Z., Guo, H.-Q. & Shan, S. (2011). *Acta Cryst.* E**67**, o3011.

Farrugia, L. J. (2012). *J. Appl. Cryst.* **45**, 849–854.

Fun, H.-K., Yip, B.-C., Tian, Y.-P., Duan, C.-Y., Lu, Z.-L. & You, X.-Z. (1996). *Acta Cryst.* C**52**, 87–89.

Low, M. L., Maigre, L. M., Tahir, M. I. M. T., Tiekink, E. R. T., Dorlet, P., Guillot, R., Ravoof, T. B., Rosli, R., Pagès, J.-M., Policar, C., Delsuc, N. & Crouse, K. A. (2016). *Eur. J. Med. Chem.* **120**, 1–12.

Omar, S. A., Chah, C. K., Ravoof, T. B. S. A., Jotani, M. M. & Tiekink, E. R. T. (2018). *Acta Cryst.* E**74**, 261–266.

Rakha, T. H. & Bekheit, M. M. (2000). *Chem. Pharm. Bull.* **48**, 914–919.

Ravoof, T. B. S. A., Crouse, K. A., Tiekink, E. R. T., Tahir, M. I. M., Yusof, E. N. M. & Rosli, R. (2017). *Polyhedron*, **133**, 383–392.

Sheldrick, G. M. (2015*a*). *Acta Cryst.* A**71**, 3–8.

Sheldrick, G. M. (2015*b*). *Acta Cryst.* C**71**, 3–8.

Spek, A. L. (2020). *Acta Cryst.* E**76**, 1–11.

Tan, S. L., Jotani, M. M. & Tiekink, E. R. T. (2019). *Acta Cryst.* E**75**, 308–318.

Tian, Y.-P., Duan, C.-Y., Lu, Z.-L., You, X.-Z., Fun, H. K. & Sivakumar, K. (1996). *Transition Met. Chem.* **21**, 254–257.

Turner, M. J., Mckinnon, J. J., Wolff, S. K., Grimwood, D. J., Spackman, P. R., Jayatilaka, D. & Spackman, M. A. (2017). *Crystal Explorer 17*. The University of Western Australia.

Westrip, S. P. (2010). *J. Appl. Cryst.* **43**, 920–925.

Yusof, E. N. M., Ravoof, T. B. S. A., Tahir, M. I. M., Jotani, M. M. & Tiekink, E. R. T. (2017). *Acta Cryst.* E**73**, 397–402.

Yusof, E. N. S. A. Md, Ravoof, T. B. S. A., Tiekink, E. R. T., Veerakumarasivam, A., Crouse, K. A., Tahir, M. I. M. & Ahmad, H. (2015). *Int. J. Mol. Sci.* **16**, 11034–11054.

supporting information

Acta Cryst. (2020). E**76**, 208-213 [https://doi.org/10.1107/S2056989020000328]

(*E*)-{[(Butylsulfanyl)methanethioyl]amino}(4-methoxybenzylidene)amine: crystal structure and Hirshfeld surface analysis

Aqilah Fasihah Rusli, Huey Chong Kwong, Karen A. Crouse, Mukesh M. Jotani and Edward R. T. Tiekink

Computing details

Data collection: *CrysAlis PRO* (Agilent, 2012); cell refinement: *CrysAlis PRO* (Agilent, 2012); data reduction: *CrysAlis PRO* (Agilent, 2012); program(s) used to solve structure: SHELXT2014 (Sheldrick, 2015*a*); program(s) used to refine structure: *SHELXL2014* (Sheldrick, 2015*b*); molecular graphics: *ORTEP-3 for Windows* (Farrugia, 2012), *DIAMOND* (Brandenburg, 2006); software used to prepare material for publication: *publCIF* (Westrip, 2010).

(*E*)-{[(Butylsulfanyl)methanethioyl]amino}(4-methoxybenzylidene)amine:

Crystal data

$C_{13}H_{18}N_2OS_2$
$M_r = 282.41$
Triclinic, $P\overline{1}$
$a = 4.7131$ (3) Å
$b = 11.6998$ (8) Å
$c = 13.5696$ (8) Å
$\alpha = 85.225$ (5)°
$\beta = 81.139$ (5)°
$\gamma = 87.379$ (5)°
$V = 736.35$ (8) Å^3
$Z = 2$
$F(000) = 300$
$D_x = 1.274$ Mg m^{-3}
Mo $K\alpha$ radiation, $\lambda = 0.71073$ Å
Cell parameters from 2643 reflections
$\theta = 3.0$–27.5°
$\mu = 0.35$ mm^{-1}
$T = 295$ K
Block, colourless
0.30 × 0.25 × 0.20 mm

Data collection

Agilent Technologies SuperNova Dual diffractometer with Atlas detector
Radiation source: SuperNova (Mo) X-ray Source
Mirror monochromator
Detector resolution: 10.4041 pixels mm^{-1}
ω scan
Absorption correction: multi-scan (CrysAlis PRO; Agilent, 2012)
$T_{min} = 0.868$, $T_{max} = 1.000$
9986 measured reflections
3395 independent reflections
2244 reflections with $I > 2\sigma(I)$
$R_{int} = 0.029$
$\theta_{max} = 27.6°$, $\theta_{min} = 3.1°$
$h = -6\rightarrow5$
$k = -15\rightarrow15$
$l = -17\rightarrow17$

Refinement

Refinement on F^2
Least-squares matrix: full
$R[F^2 > 2\sigma(F^2)] = 0.055$
$wR(F^2) = 0.174$
$S = 1.03$
3395 reflections
169 parameters
1 restraint
Primary atom site location: structure-invariant direct methods
Secondary atom site location: difference Fourier map

Hydrogen site location: mixed
H atoms treated by a mixture of independent and constrained refinement

$w = 1/[\sigma^2(F_o^2) + (0.0724P)^2 + 0.3095P]$ where $P = (F_o^2 + 2F_c^2)/3$
$(\Delta/\sigma)_{max} < 0.001$
$\Delta\rho_{max} = 0.52$ e Å^{-3}
$\Delta\rho_{min} = -0.45$ e Å^{-3}

Special details

Geometry. All esds (except the esd in the dihedral angle between two l.s. planes) are estimated using the full covariance matrix. The cell esds are taken into account individually in the estimation of esds in distances, angles and torsion angles; correlations between esds in cell parameters are only used when they are defined by crystal symmetry. An approximate (isotropic) treatment of cell esds is used for estimating esds involving l.s. planes.

Fractional atomic coordinates and isotropic or equivalent isotropic displacement parameters (Å²)

	x	*y*	*z*	U_{iso}*/U_{eq}
S1	0.33083 (16)	0.60524 (6)	0.62361 (6)	0.0687 (3)
S2	0.51025 (19)	0.46574 (8)	0.80444 (6)	0.0813 (3)
O1	1.7337 (5)	−0.06363 (18)	0.75096 (16)	0.0786 (6)
N1	0.7095 (5)	0.43553 (19)	0.62083 (18)	0.0561 (5)
H1N	0.720 (7)	0.443 (3)	0.5569 (8)	0.084 (11)*
N2	0.8729 (5)	0.35129 (18)	0.66505 (17)	0.0565 (5)
C1	0.5246 (5)	0.5021 (2)	0.6764 (2)	0.0542 (6)
C2	1.0604 (5)	0.2985 (2)	0.6052 (2)	0.0548 (6)
H2	1.0805	0.3194	0.5369	0.066*
C3	1.2420 (5)	0.2067 (2)	0.64237 (19)	0.0513 (6)
C4	1.4425 (5)	0.1496 (2)	0.5769 (2)	0.0556 (6)
H4	1.4639	0.1727	0.5090	0.067*
C5	1.6119 (5)	0.0592 (2)	0.6098 (2)	0.0564 (6)
H5	1.7446	0.0218	0.5643	0.068*
C6	1.5834 (6)	0.0250 (2)	0.7098 (2)	0.0584 (6)
C7	1.3874 (7)	0.0833 (3)	0.7765 (2)	0.0747 (9)
H7	1.3700	0.0615	0.8446	0.090*
C8	1.2198 (6)	0.1720 (3)	0.7436 (2)	0.0679 (8)
H8	1.0890	0.2098	0.7894	0.081*
C9	1.9271 (7)	−0.1303 (3)	0.6861 (3)	0.0823 (9)
H9A	1.8225	−0.1666	0.6426	0.123*
H9B	2.0223	−0.1879	0.7251	0.123*
H9C	2.0671	−0.0815	0.6468	0.123*
C10	0.2533 (8)	0.5676 (3)	0.8614 (3)	0.0891 (10)
H10A	0.1371	0.5996	0.8120	0.107*
H10B	0.1265	0.5277	0.9151	0.107*
C11	0.3805 (8)	0.6607 (3)	0.9014 (3)	0.0946 (11)
H11A	0.4893	0.7057	0.8463	0.114*
H11B	0.5150	0.6282	0.9443	0.114*
C12	0.1686 (9)	0.7410 (4)	0.9608 (3)	0.1070 (13)
H12A	0.0341	0.7741	0.9181	0.128*
H12B	0.0598	0.6964	1.0162	0.128*
C13	0.3015 (12)	0.8331 (4)	0.9999 (4)	0.1316 (18)
H13A	0.3918	0.8031	1.0558	0.197*

H13B	0.1577	0.8903	1.0211	0.197*
H13C	0.4433	0.8669	0.9486	0.197*

Atomic displacement parameters (Å²)

	U^{11}	U^{22}	U^{33}	U^{12}	U^{13}	U^{23}
S1	0.0716 (5)	0.0568 (5)	0.0760 (5)	0.0258 (3)	−0.0129 (4)	−0.0078 (3)
S2	0.0890 (6)	0.0890 (6)	0.0667 (5)	0.0326 (5)	−0.0197 (4)	−0.0151 (4)
O1	0.0860 (14)	0.0684 (13)	0.0780 (14)	0.0319 (11)	−0.0154 (11)	0.0007 (10)
N1	0.0550 (12)	0.0495 (12)	0.0640 (14)	0.0135 (10)	−0.0122 (11)	−0.0076 (10)
N2	0.0542 (12)	0.0460 (12)	0.0711 (14)	0.0134 (9)	−0.0180 (10)	−0.0076 (10)
C1	0.0493 (13)	0.0468 (14)	0.0676 (16)	0.0048 (11)	−0.0119 (11)	−0.0089 (12)
C2	0.0512 (14)	0.0495 (14)	0.0649 (15)	0.0073 (11)	−0.0123 (12)	−0.0088 (12)
C3	0.0483 (13)	0.0432 (13)	0.0643 (15)	0.0080 (10)	−0.0135 (11)	−0.0109 (11)
C4	0.0558 (15)	0.0514 (15)	0.0588 (15)	0.0078 (11)	−0.0084 (12)	−0.0061 (12)
C5	0.0498 (14)	0.0497 (15)	0.0685 (17)	0.0104 (11)	−0.0036 (12)	−0.0130 (12)
C6	0.0574 (15)	0.0506 (15)	0.0675 (17)	0.0120 (12)	−0.0141 (12)	−0.0055 (12)
C7	0.090 (2)	0.075 (2)	0.0570 (16)	0.0288 (16)	−0.0126 (15)	−0.0091 (14)
C8	0.0734 (18)	0.0662 (18)	0.0621 (17)	0.0249 (14)	−0.0063 (14)	−0.0151 (13)
C9	0.082 (2)	0.070 (2)	0.093 (2)	0.0347 (17)	−0.0182 (18)	−0.0072 (17)
C10	0.079 (2)	0.111 (3)	0.076 (2)	0.027 (2)	−0.0061 (17)	−0.0252 (19)
C11	0.079 (2)	0.089 (3)	0.118 (3)	0.0138 (19)	−0.013 (2)	−0.032 (2)
C12	0.099 (3)	0.115 (3)	0.108 (3)	0.029 (2)	−0.012 (2)	−0.040 (3)
C13	0.162 (5)	0.099 (3)	0.125 (4)	0.004 (3)	0.017 (3)	−0.033 (3)

Geometric parameters (Å, º)

S1—C1	1.662 (3)	C7—C8	1.363 (4)
S2—C1	1.745 (3)	C7—H7	0.9300
S2—C10	1.793 (3)	C8—H8	0.9300
O1—C6	1.359 (3)	C9—H9A	0.9600
O1—C9	1.420 (4)	C9—H9B	0.9600
N1—C1	1.330 (3)	C9—H9C	0.9600
N1—N2	1.378 (3)	C10—C11	1.450 (5)
N1—H1N	0.859 (10)	C10—H10A	0.9700
N2—C2	1.278 (3)	C10—H10B	0.9700
C2—C3	1.449 (3)	C11—C12	1.524 (5)
C2—H2	0.9300	C11—H11A	0.9700
C3—C4	1.382 (3)	C11—H11B	0.9700
C3—C8	1.389 (4)	C12—C13	1.446 (6)
C4—C5	1.382 (4)	C12—H12A	0.9700
C4—H4	0.9300	C12—H12B	0.9700
C5—C6	1.371 (4)	C13—H13A	0.9600
C5—H5	0.9300	C13—H13B	0.9600
C6—C7	1.387 (4)	C13—H13C	0.9600
C1—S2—C10	103.87 (16)	O1—C9—H9A	109.5
C6—O1—C9	118.4 (2)	O1—C9—H9B	109.5

C1—N1—N2	120.6 (2)	H9A—C9—H9B	109.5
C1—N1—H1N	119 (2)	O1—C9—H9C	109.5
N2—N1—H1N	120 (2)	H9A—C9—H9C	109.5
C2—N2—N1	115.6 (2)	H9B—C9—H9C	109.5
N1—C1—S1	120.9 (2)	C11—C10—S2	114.0 (3)
N1—C1—S2	112.76 (19)	C11—C10—H10A	108.7
S1—C1—S2	126.35 (16)	S2—C10—H10A	108.7
N2—C2—C3	120.9 (2)	C11—C10—H10B	108.7
N2—C2—H2	119.6	S2—C10—H10B	108.7
C3—C2—H2	119.6	H10A—C10—H10B	107.6
C4—C3—C8	117.8 (2)	C10—C11—C12	115.3 (3)
C4—C3—C2	120.4 (2)	C10—C11—H11A	108.4
C8—C3—C2	121.8 (2)	C12—C11—H11A	108.4
C3—C4—C5	121.7 (2)	C10—C11—H11B	108.4
C3—C4—H4	119.1	C12—C11—H11B	108.4
C5—C4—H4	119.1	H11A—C11—H11B	107.5
C6—C5—C4	119.6 (2)	C13—C12—C11	114.1 (4)
C6—C5—H5	120.2	C13—C12—H12A	108.7
C4—C5—H5	120.2	C11—C12—H12A	108.7
O1—C6—C5	125.1 (2)	C13—C12—H12B	108.7
O1—C6—C7	115.7 (3)	C11—C12—H12B	108.7
C5—C6—C7	119.1 (2)	H12A—C12—H12B	107.6
C8—C7—C6	120.9 (3)	C12—C13—H13A	109.5
C8—C7—H7	119.5	C12—C13—H13B	109.5
C6—C7—H7	119.5	H13A—C13—H13B	109.5
C7—C8—C3	120.8 (3)	C12—C13—H13C	109.5
C7—C8—H8	119.6	H13A—C13—H13C	109.5
C3—C8—H8	119.6	H13B—C13—H13C	109.5

C1—N1—N2—C2	−174.5 (2)	C9—O1—C6—C7	176.9 (3)
N2—N1—C1—S1	178.96 (18)	C4—C5—C6—O1	178.8 (2)
N2—N1—C1—S2	−2.2 (3)	C4—C5—C6—C7	−1.0 (4)
C10—S2—C1—N1	179.3 (2)	O1—C6—C7—C8	−178.5 (3)
C10—S2—C1—S1	−1.9 (2)	C5—C6—C7—C8	1.4 (5)
N1—N2—C2—C3	−178.8 (2)	C6—C7—C8—C3	−0.3 (5)
N2—C2—C3—C4	179.5 (2)	C4—C3—C8—C7	−1.1 (4)
N2—C2—C3—C8	0.3 (4)	C2—C3—C8—C7	178.1 (3)
C8—C3—C4—C5	1.5 (4)	C1—S2—C10—C11	−102.1 (3)
C2—C3—C4—C5	−177.8 (2)	S2—C10—C11—C12	−173.2 (3)
C3—C4—C5—C6	−0.4 (4)	C10—C11—C12—C13	180.0 (4)
C9—O1—C6—C5	−3.0 (4)		

Hydrogen-bond geometry (Å, º)

*Cg*1 is the centroid of the (C3–C8) ring.

D—H···*A*	*D*—H	H···*A*	*D*···*A*	*D*—H···*A*
N1—H1*N*···S1^{i}	0.86 (1)	2.61 (2)	3.425 (3)	160 (3)

C9—H9*C*···*Cg*1^{ii}	0.96	2.98	3.748 (4)	138

Symmetry codes: (i) −*x*+1, −*y*+1, −*z*+1; (ii) *x*+1, *y*, *z*.